DENTAL MATERIALS 35 (2019) 457–467

Available online at www.sciencedirect.com

ScienceDirect

journal homepage: www.intl.elsevierhealth.com/journals/dema

Antimicrobial and anti-inflammatory drug-delivery systems at endodontic reparative material: Synthesis and characterization

Marla Cuppini[a], *Kelly Cristine Zatta*[b], *Letícia Boldrin Mestieri*[c], *Fabiana Soares Grecca*[c], *Vicente Castelo Branco Leitune*[a], *Sílvia Stanisçuaski Guterres*[b], *Fabrício Mezzomo Collares*[a,*]

[a] *Department of Conservative Dentistry, Dental Materials Laboratory, School of Dentistry, Universidade Federal do Rio Grande do Sul, Rua Ramiro Barcelos 2492, Porto Alegre, Rio Grande do Sul 90035-003, Brazil*
[b] *Cosmetology Laboratory, School of Pharmaceutical Sciences, Universidade Federal do Rio Grande do Sul, Av. Ipiranga 2752, Porto Alegre, Rio Grande do Sul 90610-000, Brazil*
[c] *Department of Conservative Dentistry, Endodontics, School of Dentistry, Universidade Federal do Rio Grande do Sul, Rua Ramiro Barcelos 2492, Porto Alegre, Rio Grande do Sul 90035-003, Brazil*

ARTICLE INFO

Article history:
Received 5 July 2018
Received in revised form
5 December 2018
Accepted 3 January 2019

Keywords:
Microspheres
Amoxicillin
Nanocapsules
Indomethacin
Drug delivery systems
Bioactivity
Biocompatibility

ABSTRACT

Objective. The aim of this study was to synthesize and characterize an experimental endodontic paste.

Methods. An experimental endodontic paste (EX) was characterized by its particle size, zeta potential, drug content and morphology. The powder of EX is composed of amoxicillin microspheres, calcium tungstate and α-tricalcium phosphate, mixed with an indomethacin nanocapsules suspension. Ultracal® (Ultradent), an iodoform-based paste (GP) and the EX were evaluated by its physical properties (flow, film thickness and radiopacity). The cytocompatibility was performed by MTT and SRB-colorimetric assays; the cell-migration was tested with scratch assay and cell-ability to remineralization with ALP and Alizarin Red S, with fibroblastic cell line. The antibacterial activity was assessed by the formation of inhibition zones and against planktonic bacteria.

Results. The EX and UL flow achieved ISO6876 standard, and GP was lower than 17 mm. All pastes achieved the film thickness required. Radiopacity was equivalent to 1.81 ± 0.25 mmAl for EX, which did not differ from GP group 1.39 ± 0.33 mmAl ($p > 0.05$). The UL presented 3.04 ± 0.33 mmAl. The values for SRB showed better citocompatibility in comparison with MTT for all materials. The ALP activity and formation of mineralized nodules demonstrated the remineralization potential for UL and EX. Cell migration showed continuous wound closure until complete cell healing, however, the EX accelerated the process ($p < 0.05$). The EX showed the greatest inhibition zone ($p < 0.05$) and was the only group with antibacterial activity against planktonic bacteria.

Significance. The synthesized endodontic paste demonstrated reliable physical and biological properties and could be a promising material for periapical tissue repair.

* *Corresponding author.*
E-mail address: fabricio.collares@ufrgs.br (F.M. Collares).
https://doi.org/10.1016/j.dental.2019.01.002

1. Introduction

The success of endodontic treatment depends on the reduction or elimination of bacteria [1]. The chemomechanical preparation reduces the number of microorganisms; however, this therapy does not eliminate all the bacteria [2]. Calcium hydroxide ($Ca(OH)_2$) has been advocated as intracanal medication for this purpose due to its elevated pH of 12.5 which can lead to protein denaturation and damage of the bacterial cytoplasmic membrane [3].

In primary teeth, treatment allows maintaining the affected tooth in a functional state, free of infection, until physiological exfoliation and replacement by the permanent successor, thereby avoiding premature loss [4]. The microorganisms found in the root canal of the primary teeth are similar to those in the root canals of permanent teeth. *Enterococcus faecalis* was found in almost 15% of deciduous teeth [5], however, this microorganism shows resistance to $Ca(OH)_2$ [6].

The association of iodoform, camphorated paramonochlorophenol, corticoid, and antibiotic paste to obtain disinfection and facilitate tissue repair has shown some antimicrobial action against microorganisms found in endodontic infection in primary teeth [7]. Moreover, it has been reported the toxicity of the camphorated paramonochlorophenol component [8].

On the other hand, the endodontic regeneration procedures have returned the use of various antibiotic mixtures as intracanal medicaments such as triple antibiotic paste containing metronidazole, ciprofloxacin, and minocycline and became an alternative conservative treatment option for young permanent teeth with immature roots [9]. However, minocycline may cause tooth discoloration and binds to calcium ions via chelation to form an insoluble complex [10,11].

To avoid such complications, endodontic materials have been developed with bioactive attributes such as antibacterial [12] and remineralizing [13] properties to enhance disinfection and apical tissues repair. Patients in dental clinics with endodontic-related problems still systemically take a high level of drugs to assure efficacy of the proposed treatment [14], but as consequence, drug resistance, toxicity and adverse effects may appear [15,16]. Thus, for the development of bioactive materials, it should be considered the composition of drug active components, along with a carrier with high biocompatibility and sustained release of the active components [17]. An alternative strategy could be the use of polymeric microspheres and nanocapsules that contain pharmacological components, such as indomethacin and amoxicillin, promoting effective controlled drug release [18,19]. The pharmacological response to a drug is related to its concentration at the local site of action [18] and improved drug efficacy and bioavailability are obtained from encapsulation even with lower therapeutic doses [20,21].

The bioactive devices of drug carrier systems may have micro or nanometric dimensions. The nanocapsules and microspheres differ in composition and structural organization [16]. A polymeric wall disposed around an oily core containing the drug constitutes the nanocapsules, for this type of particle lipophilic drugs are usually contained [16]. On the other hand, microspheres do not present oil in their composition, and are formed by a polymeric matrix, where the drug can be retained or adsorbed on the surface of the polymer network, commonly used for hydrophilic drugs [18–20]. The nanotechnology associated with bioactive materials aim to ameliorate the repair process, presenting certain level of cell bioactivity and not being inert to the microenvironment [22].

This study proposes a new method of delivering active agents to regions with difficult access in Dentistry, as it is in endodontic treatment. Therefore, the aim of this study was to evaluate the physical properties, biocompatibility, cell differentiation and bioactivity of an experimental endodontic paste allied to nanotechnology.

2. Materials and methods

2.1. *Particles synthesis*

Preparation of nanocapsule suspension (IndOH-NCs)

Nanocapsules (NC) loaded with indomethacin (IndOH) were prepared by mixing an organic phase with Eudragit® S100 (Evonik Industries AG Pharma Polymers & Services, Kirschenallee, Darmstadt, Germany), poly (MMA-co-MAA) (0.50 g), indomethacin (Sigma–Aldrich Chemical, Inc., St. Louis, MO, USA) (0.05 g), medium chain triglycerides oil (Alpha Química, Porto Alegre, RS, Brazil) (0.81 mL), and sorbitan monoestearate (Sigma–Aldrich Chemical, Inc., St. Louis, MO, USA) (0.19 g) dissolved in acetone (Nuclear, São Paulo, SP, Brazil) (125 mL) under magnetic stirring for 30 min (at 37 °C) [23,24]. The organic phase was injected in an aqueous phase composed by polysorbate 80 (Henrifarma, Sao Paulo, SP, Brazil) (0.385 g) and ultrapure water (200 mL), while stirring. Solvents were removed by reduced pressure (Rotavapor R-114, Büchi, Flawil, Switzerland), coupled to a B-740 recirculating chiller (Buchi, Flawi, Switzerland), and a U-700 vacuum pump (Buchi, Flawi, Switzerland). After solvent evaporation, the suspensions were concentrated to the final volume of 50 mL.

Preparation of microspheres powder (AMX-MS)

The amoxicillin (Spengler Pharmacy, Porto Alegre, RS, Brazil) (AMX) microspheres (MS) were produced by a spray-drying technique. Eudragit® S100, poly (MMA-co-MAA) (0.6 g) and sorbitan monoestearate (0.038 g) were dissolved in acetone (27 mL) and absolute ethanol (Nuclear, São Paulo, SP, Brazil) (10 mL) composing the organic solution. An aqueous phase was prepared with amoxicillin (0.3 g) and polysorbate 80 (0.077 g) dissolved in 73 mL of ultra pure water and 10 mL of absolute ethanol, until a clear solution was formed under continuous magnetic stirring at 37 °C. The organic solution was injected into the aqueous solution (solution A). It was prepared a dispersion of hydroxypropyl methylcellulose (METHOCEL™ – HPMC – F4M, Dow Pharma & Food Solutions, Midland, MI, USA) with ultrapure water (0.9 g of HPMC and 100 mL of ultrapure water). The solution A was injected with a funnel into the HPMC dispersion. The resultant solution was spray dried using a Mini-Spray Dryer B-290 (Buchi, Flawi, Switzerland) coupled to a dehumidifier (B-292, Buchi, Flawi, Switzerland) using the

following parameters: feed pump rate of 5.0 mL min^{-1}, 100% aspiration, 0.7 mm nozzle, atomization air at 819 L h^{-1}, and an inlet temperature of 90 °C with a resulting outlet temperature of approximately 45 °C.

2.2. Characterization of the synthesized particles

2.2.1. Particle size distribution

The mean diameter ($D_{4,3}$) and span value of the indomethacin nanocapsules solution and amoxicillin microspheres powder were evaluated by laser diffraction (n = 3) (LD, Mastersizer 2000® 5.61, Malvern Instruments, UK). The AMX-MS was analyzed with a dry unit dispersion (Scirocco module, Malvern Instruments, Worcestershire, UK) to warrant a dry way analysis. The refractive indexes used for samples were 1.336 for AMX-MS and 1.380 for IndOH-NC. The laser obscuration was set to 2%. The results were analyzed by Mastersizer 2000® 5.61 software.

2.2.2. Zeta potential

The zeta potential of the indomethacin nanocapsules suspension (n = 3) was determined by electrophoretic mobility (Zetasizer Nano ZS®, Malvern, UK), using 0.1 M NaCl as the dispersant (1:40 v/v). The results were analyzed by Zetasizer 7.11 software program.

2.2.3. Morphological analysis

The morphology of IndOH-NC was analyzed by transmission electron microscopy (TEM). The samples were diluted in ultrapure water (1:10 v/v), and one drop of the dilution was placed on a grid (Formvar-carbon support films 400 mesh) for 5 min. After that, a drop of uranyl acetate (2% w/v) was also disposed. The grid was placed on TEM (TEM, JEM1200 Exll, Jeol, Tokyo, Japan) operated at 80 kV with magnifications of 200× and 300×. Dried amoxicillin microspheres (0.01 g) were processed using gold-sputter coating and submitted to scanning electron microscopy (SEM, JSM 6060, Jeol, Tokyo, Japan) at an accelerating voltage of 15 kV and 3.5-nm resolution.

2.2.4. Drug content

The drug quantification of the AMX-MS and IndOH-NC was assayed by high-performance liquid chromatography (HPLC-UV, Perkin Elmer Series 200), the analysis parameters are listed in Table 1.

2.3. Formulation of the experimental endodontic paste

To each 1 g of amoxicillin microspheres it was added 0.2 g of α-TCP, prepared as previous described [25], and 0.4 g of $CaWO_4$ (Sigma–Aldrich Chemical, Inc., St. Louis, MO, USA) to compose the powder formulation. The proportion of the mixture is 0.4 mL of IndOH-NC suspension to 0.6 g of the formulated powder.

2.4. Characterization and biological properties of endodontic pastes

The materials tested were the experimental paste (EX), a calcium hydroxide-based material (UL) (Ultracal® XS, Ultradent Products Inc. South Jordan, UT, EUA) and an iodoform-based paste (GP – Guedes-Pinto alike) prepared at room temperature. The proportion ratio of GP alike paste was: 23.8% neomycin sulfate and prednisolone acetate, 7.0% of camphorated paramonochlorophenol and 69.2% of iodoform.

2.4.1. Flow

Flow test was conducted according to ISO 6876:2012 (n = 3). A 0.05 mL aliquot of the freshly mixed paste was placed on glass plates (40 × 5 mm). At 180 ± 5 s after the mixing, another equal plate with a mass of 20 ± 2 g and a load of 100 g was applied on top of the material. Ten minutes after, the load was removed, and the major and minor diameters of the compressed paste were measured.

2.4.2. Film thickness

Film thickness test was conducted according to ISO 6876:2012 (n = 3). Two glass plates (5 mm thick and 10 mm side) were placed together, and their combined thickness was measured (F1). Then, 0.05 mL of experimental paste was placed at the center of the plates and 150 N load was applied vertically on the top. Ten minutes after mixing, the combined thickness of the two glass plates and the interposed paste film was measured (F2). The difference between F1 and F2 was used to calculate the mean film thickness in three measurements.

2.4.3. Radiopacity

Radiopacity was assessed according to ISO 6876:2012. Radiographic images of specimens (n = 5) 10.0 ± 0.1 mm diameter × 1.0 ± 0.01 mm thickness were obtained with a 400 mm focus-film distance using a phosphor plate digital system (VistaScan, Dürr Dental GmbH & Co. KG, Germany) exposed by 0.2 s at 70 kV and 8 mA (Spectro 70×, Dabi Atlante Ltda, Brazil). An aluminium step-wedge having a thickness range from 1.0 to 8.0 mm was simultaneously exposed. The means and standard deviations of the grey levels of the aluminium step-wedge and the specimens were obtained with ImageJ analysis (Wayne Rasband, EUA) in a standardized area of 2 mm^2.

2.4.4. In vitro antibacterial behavior

2.4.4.1. Agar diffusion test (ADT). The surface of brain-heart infusion agar (BHI agar, Sigma–Aldrich Chemical Co., St. Louis, Missouri, USA) in five Petri dishes were inoculated with 0.3 mL of a bacterial suspension, obtained from a 10^{-4} serial dilution of an adjusted *E. faecalis* culture (ATCC 29212, Rockville, USA). One Petri dish did not receive the bacterial suspension to assure the sterilization of the BHI agar and one did not receive the materials and aimed to control the contamination of the inoculate. Three discs (n = 3) of 10 ± 0.1 mm diameter and 1.0 ± 0.01 mm thick of the experimental groups were placed on the agar surface of three different plates and then all plates were incubated at 36 °C for 24 h, under aerobic conditions. The inhibition zone around each sample was measured by the same operator in two perpendicular locations with a digital caliper. The size of the inhibition zone was calculated as follows: size of inhibition zone = diameter of halo – diameter of specimen.

2.4.4.2. Evaluation of antibacterial activity against planktonic bacteria. The materials were manipulated (1 g) and placed on the bottom of the sterile 96-well plate (n = 3), in each well it

Table 1 – Parameters for drug content analysis.

Parameters	Amoxicillin microspheres	Indomethacin nanocapsules
Linearity	20–60 mg mL^{-1} (r = 0.99)	1.5 to 15 mg mL^{-1} (r = 0.99)
Detection (λ)	230 nm	280 nm
Column	C18 Phenomenex (5 μm, 250 mm × 4.6 mm) and guard column (Phenomenex)	C18 Phenomenex (5 μm, 250 mm × 4.6 mm) and guard column (Phenomenex)
Mobile phase	H_2SO_4 0,005 M and acetonitrile (80:20) solution, pH 4.5 adjusted with acetic acid.	Acetonitrile and water (60:40) solution, pH 4.5, adjusted with acetic acid.
Injection volume	20 μL	20 μL

was added 900 μL of brain-heart infusion broth (BHI broth, Sigma–Aldrich Chemical Co., St. Louis, Missouri, USA) with 100 μL of a suspension of an overnight broth culture of *E. faecalis*. The plate was incubated with culture medium with 4.12×10^7 CFU/mL of bacteria at 37 °C for 24 h. A negative control (n = 3) was also incubated with the experimental groups, with 900 μL of BHI broth and 100 μL of *E. faecalis*. For the first dilution, 100 μL of each well was diluted in 900 μL of saline solution (0.9%) until the 10^{-6} dilution. Two drops (20 μL each) of each dilution were platted in BHI agar Petri dishes and incubated for 48 h at 37 °C and the number of colony forming units (CFUs) was counted at 10^{-4} serial dilution using optical microscopy and transformed to log CFU/mL.

2.4.5. *In vitro cell behavior*

Fibroblastic (3T3-L1) cell line prevenient from Rio de Janeiro Cell Bank (Banco de Células do Rio de Janeiro – BCRJ, Rio de Janeiro, Brazil) were grown as a monolayer culture in T-75 flasks (Corning, Union City, USA) in Dulbecco Modified Eagle Medium (DMEM – Sigma/Aldrich, St. Louis, USA) supplemented with 10% foetal bovine serum (FBS – Thermo Fisher Scientific, USA), penicillin (100 IU/mL) (Thermo Fisher Scientific, USA), and streptomycin (100 mg/mL) (Thermo Fisher Scientific, USA) until confluence. The cells were subcultured twice a week at 37 °C, 95% humidity and 5% CO_2. To asses cell behavior, conditioned medium from freshly-mixed and setting, all materials were prepared at room temperature and, thereafter, each material was individually placed in 4 wells of a 12-well plate (TPP, Techno Plastic Products, Zollstrasse, Trasadingen, Switzerland). The materials were compacted using a sterile cotton swab until it was homogenously distributed, occupying the whole well surface with an area of 3.8 cm^2, and immediately covered with 6 mL of culture medium. The extraction of the different materials' was performed in sterile chemically inert laminar flow using aseptic techniques, in accordance with ISO 10993-12. Another 12-well plate was filled with materials and kept in an incubator at 37 °C, 95% humidity and 5% CO_2 during 24 h for the initial setting time of the materials, after this period, the samples were exposed to ultraviolet light (UV) in a laminar flow for 30 min to prevent contamination, then, the wells were covered with 6 mL of culture medium, which is within the recommended range of 0.5–6.0 cm^2/mL suggested by ISO 10993-12:2012.

2.4.5.1. *Cell proliferation assays*. The proliferation rate of fibroblasts (3T3-L1) cells was estimated by two assays, MTT and SRB. The cells (1×10^4/well) were seeded in 96-well plate and stored in a humidified atmosphere of 5% CO_2 and 95% air at 37 °C until 90% confluence. After 90% confluence, cells were treated with 100 μL the conditioned medium (dilutions of 10, 5 and 1%) for 24 h. The results were expressed as percentage of proliferation in relation to the control group (cells cultured in the absence of any material used).

MTT tetrazolium salt colorimetric assay

Four hours prior the 24 h period it was added 10 μL of 3-[4,5-dimethylthiazol-2-yl]-2,5-diphenyltetrazolium bromide (MTT) solution (0.5 mg/mL) to each well. The plates were maintained in the incubator for completing the 24 h period. Then, the medium was remove, and it was added 100 μL of acidic isopropanol (HCl 4N) to release formazan synthesized in the mitochondria. Optical density was measured at a wavelength of 570 nm in a spectrophotometer (Multiskan^{TM} GO – Thermo Fischer Scientific Inc., Waltham, MA, USA).

Sulforhodamine B colorimetric assay

After completing the period, the medium was removed and cells were fixed with 50 μL trichloroacetic acid 50% (Sigma Aldrich, St. Louis, EUA). The wells were then washed with distilled water and stained with 50 μL SRB 0.4% (Sigma–Aldrich, St. Louis, MO) in 1% acetic acid for 30 min. Subsequently, the wells were washed in 1% solution of acetic acid. Plates were dried at room temperature and 100 μL of Tris solution 10 mm/mol was added to each well. The plates were measured at a wavelength of 560 nm in a microplate spectrophotometer (Multiskan^{TM} GO – Thermo Fischer Scientific Inc, Waltham, MA, USA).

2.4.5.2. *Bioactivity assays*. Bioactivity of fibroblasts (3T3-L1) cells was estimated by three different tests: alkaline phosphatase activity (ALP), Alizarin Red S mineralization and a wound-healing (scratch) assay. For all tests, cells (1×10^4) were seeded in in 24-well plates with culture medium supplemented with 10% fetal bovine serum (FBS), penicillin and streptomycin (10,000 U/mL) and stored in a humidified atmosphere of 5% CO_2 and 95% air at 37 °C until 90% confluence. After 90% confluence, cells were treated with experimental conditioned medium prepared as previous mentioned, at 10% concentration.

Alkaline phosphatase (ALP) activity

ALP activity was implemented utilizing an ALP assay kit (Labtest; Lagoa Santa, MG, Brazil). The cells were incubated in conditioned medium and tested after 7 and 14 days to investigate osteogenic differentiation of fibroblasts. The conditioned medium was replaced every 3–4 days on the 24-well-plates. After completing periods of exposure, cells were fixed with 1% Tris for 20 min, the attached fibroblastic cells were rinsed with PBS 1× and immersed in 1 mL sodium dodecyl sulfate solu-

tion (SDS, Sigma–Aldrich Chemical, Inc. St. Louis, MO, USA) for 30 min at room temperature. Then, it was followed strictly the instructions proposed on the reagent kit to release ALP activity to the medium. The reaction was terminated with a stop solution and the absorbance of *p*-nitrophenol was measured at 590 nm (Multiskan^{TM} GO – Thermo Fischer Scientific Inc., Waltham, MA, USA), and ALP activity was calculated as follows: Alkaline Phosphatase (U/L) = $A_{test}/A_{standard}$ X 45.

Alizarin Red S (ARS) mineralization assay

Alizarin Red S was used to quantify cell mineralization. After 7 and 14 days, cells were rinsed with PBS and fixed with formaldehyde 10% at room temperature. After 20 min, it was added 500 μL of Alizarin Red S 2% aqueous solution to each well (pH 4.2) for 30 min and then, plates were rinsed with distilled water. Stained monolayers were observed using an inverted microscope (Axiovert 100, Carl Zeiss, Jena, Germany) with 4.2″ magnification where images were taken with a digital camera (Sony Cyber-Shot W800, SONY Corporation, Tokyo, Japan). Mineralized nodules quantification was calculated using ImageJ software (National Institutes of Health, Bethesda, MD).

Scratch wound healing assay

Cells (2×10^5/well) were seeded in a 24-well plate and after 90% confluence, the monolayer of fibroblasts (3T3-L1) was scratched cross-shaped-like with a P200 pipette tip (TPP, Techno Plastic Products, Trasadigen, Switzerland) and washed with 1 mL PBS. The wounded monolayer of cells was allowed to heal in the presence of the conditioned medium (n = 3). Photographs were taken every 6-h with the help of an inverted microscope (Carl Zeiss Microscopy Gmbh, Göttingen, Germany) at 10″ magnification coupled with a digital camera (Sony Cyber-Shot W800, SONY Corporation, Tokyo, Japan). Relative rates of wound closure were measured and expressed as percentage of the initial wound length at baseline (time of the scratch = 0) until complete wound healing. Rates were compared to control and analyzed by ImageJ (NIH, Bethesda, MD, USA).

2.5. *Statistical analysis*

Descriptive analysis was performed for characterization assays. The normality of all data was analyzed by Shapiro–Wilk. One-way ANOVA was used to compare different groups for radiopacity, film thickness, flow and antimicrobial planktonic test, followed by Tukey *post hoc* test. The agar diffusion antimicrobial test was performed with a Student t-test. The cell assays were analyzed by two-way ANOVA and Tukey *post hoc test*. All tests were performed considering a level of significance of 5% (GraphPad Prism software, version 7.0, GraphPad Software, Inc., San Diego, CA, USA) (Table 2).

3. Results

The IndOH-NCs suspensions had monomodal particle size distribution, with mean particle size ($D_{4,3}$) of 162 ± 7.5 nm and Span value of 1.177 ± 0.22, according to laser diffraction analysis. The zeta potential was negative for all tested batches (−21.3 ± 4.61 mV). Analysis of IndOH-NC in TEM (Fig. 1) showed indomethacin-loaded NCs with spherical morphology and nanometric dimensions. It was possible to see a polymeric capsule around IndOH-NCs. The load content of the indomethacin was 1 mg mL^{-1} ± 0.02, verified by HPLC. For AMX-MS, the mean particle size ($D_{4,3}$) was 1.604 ± 0.08 μm and Span value of 0.829 ± 0.07. Analysis of AMX-MS powder in SEM (Fig. 2) showed mainly spherical micrometric particles, which presented smoother surface and some invaginations. The load content of the amoxicillin was 163 ± 2.10 mg g^{-1} verified by HPLC.

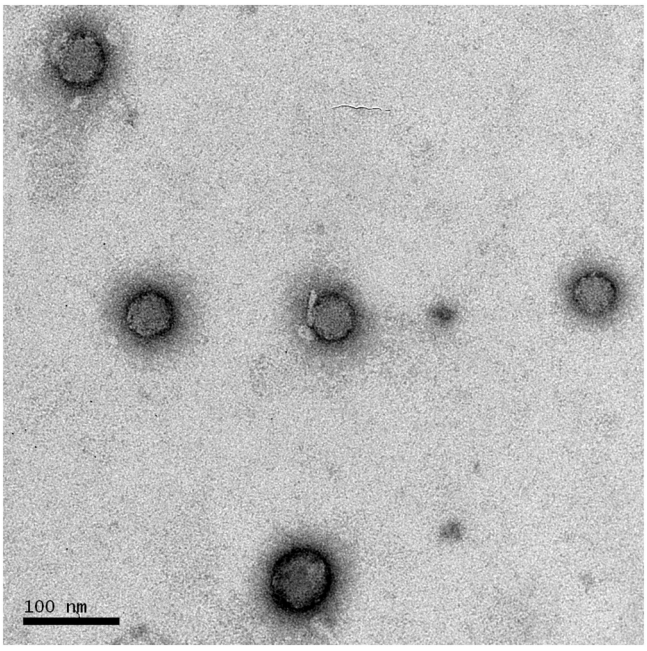

Fig. 1 – SEM image AMX-MS spray-dried formulations under 20.000× magnification.

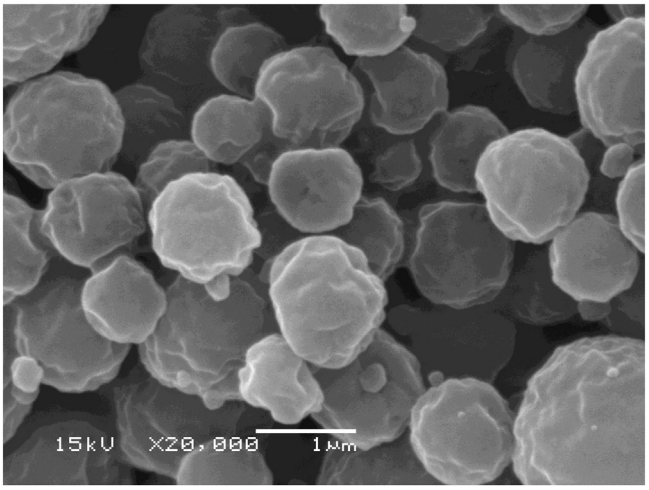

Fig. 2 – TEM images of IndOH-NC under 250.000× magnification.

Table 2 – Particles analysis.

Particle	Particle size	Span	Drug content	Zeta potential
IndOH-NC	162 ± 7.5 nm	1.177 ± 0.22	1 ± 0.02 mg mL^{-1}	−21.3 ± 4.61 mV
AMX-MS	1.604 ± 0.08 μm	0.829 ± 0.07	163 ± 2.10 mg g^{-1}	–

The physical and antimicrobial characterization of the materials tested is presented in Table 3. Mean flow of the experimental endodontic paste was 18.56 ± 0.29 mm, for UL group was 22.89 ± 0.8 mm and for the GP group was 15.61 ± 0.4 mm. The mean film thickness found was 33 ± 0.01 μm for EX and UL group, and 40 ± 0.01 μm for GP group. Radiopacity was equivalent to 1.81 ± 0.25 mmAl for the experimental paste, which did not differ from GP group, 1.39 ± 0.33 mmAl ($p > 0.05$). The UL paste presented higher radiopacity (3.04 ± 0.33 mmAl) than GP and Ex groups ($p < 0.05$).

The results for Agar Diffusion Test showed that all materials tested formed inhibition zones, except for the Ultracal® XS group. The experimental endodontic paste presented higher inhibition halo than GP and UL groups ($p < 0.05$), ranging from 18.65 to 21.48 mm. The GP group presented an inhibition halo ranging from 9.36 to 12.21 mm. For the antibacterial activity against planktonic bacteria the experimental paste was the only group to present antibacterial effect ($p < 0.05$). The GP and UL groups showed no significant difference to negative control group ($p > 0.05$).

The cell proliferation tests showed acceptable results regarding citocompatibility for all groups according to ISO 10993-5 standards. The experimental material at 10% conditioned medium presented 187.03% of viability after setting on SRB test, which was the highest result for this assay ($p < 0.05$). For the osteogenic potential assays, the ARS (Fig. 4) revealed statistically lower results of mineralized nodules formation for GP group. UL and EX showed comparable area fraction of mineralized nodules with no statistical difference ($p > 0.05$). The ALP assay (Fig. 5) showed greater activity after 14 days of cell culture. For the scratch wound-healing model, treatment with all materials promoted migration in treated cells as it is shown in Fig. 6. It has been shown in this study that the experimental paste accelerated the cellular migration of fibroblastic cell line in comparison to other materials tested ($p < 0.05$).

4. Discussion

The development of bioactive materials are required due to its participation in the dynamic activity occurring at the local repair process and thus, biomaterials for periapical tissue repair is a demand in dental clinics. Due to anatomical factors of teeth with open apex and primary teeth, the disinfection and endodontic treatment process may be hinder. The outcomes of this study indicate that this experimental endodontic paste has potential to be used as an intra-canal dressing for regenerative treatment and filling material in primary teeth.

The IndOH-NC suspension showed homogeneous macroscopic condition and presented a milky white aspect with the presence of Tyndall effect, produced by interfacial deposition of a preformed polymer. The AMX-MS showed a fine particle powder formation. The newly developed material presented reliable physical properties, antibacterial efficacy against *E. faecalis* and suitable cytocompatibility and bioactivity. In this study, a novel reparative endodontic material was successfully synthesized.

The IndOH-NC suspension presented nanometric size and low polydispersity index, as expected for this kind of formulation formed by the diffusion of the organic solvent in the aqueous phase interface [23,26]. The TEM image in Fig. 1 showed spherical morphology in accordance with previous studies with indomethacin polymeric encapsulation [24]. The AMX-MS prepared by the spray-drying technique showed formation of spherical particles in the micrometric range. The polysorbate 80 present in the AMX-MS is able to prevent particle coalescence or aggregation due to a steric stabilization effect as it is seen in Fig. 2 and by its low polydispersity index result [26]. The synthesized AMX-MS in addition to α-TCP and $CaWO_4$ was able to formulate an easy handling paste with the IndOH-NC suspension, which showed adequate flow and film thickness, according to ISO6876:2012.

The rheological behavior of the experimental paste showed the ability to create a thin film and adequate flow, which can promote the wetting of the root canal surface [27], this results for physical properties allow the penetration of the material inside dentinal tubules, and materials with antimicrobial effect could prevent the bacterial growth in the canal system [28]. The Ultracal paste showed all physicochemical properties tested in accordance with ISO 6876 specifications, however, did not presented antibacterial activity. The penetration of bioactive materials and effective permeation of ions

Table 3 – Mean ± SD of film thickness, flow, radiopacity, inhibition zone and bacterial growth of materials tested.

Group	Film thickness (μm)[a]	Flow (mm)[a]	Radiopacity (mmAl)[a]	Inhibition zone (mm)	Bacterial growth (log CFU/mL)
Experimental paste	33 ± 0.01^{B}	18.56 ± 0.29^{B}	1.81 ± 0.25^{B}	19.99 ± 1.42^{A}	7.13 ± 0.12^{B}
Ultracal XS paste	33 ± 0.01^{B}	22.89 ± 0.8^{A}	3.04 ± 0.33^{A}	0 ± 0	7.304 ± 0.02^{AB}
Guedes-Pinto paste	40 ± 0.01^{A}	15.61 ± 0.4^{C}	1.39 ± 0.31^{B}	11.07 ± 1.5^{B}	7.43 ± 0.15^{AB}
Negative control	–	–	–	–	7.5 ± 0.11^{A}

Different capital letters indicate significant difference between columns.

[a] ISO 6876:2012 recommendations: film thickness less than 50 μm, flow of at least 17 mm and 3 mmAl of radiopacity.

is possible to be achieved with the experimental endodontic paste, which presented properties to wet the root canal surface associated with antimicrobial activity. The interaction with periapical tissues forming a mineralized barrier at the foramen is a result of improved repair process of periapical area attained with truly bioactive materials [29]. Although the radiopacity of the EX and GP paste did not reach the requirements of ISO 6876, the values obtained are comparable with other calcium hydroxide-based materials [30].

For a nanosuspension to be considered stable the zeta potential of the suspension should be distant from 0, a desired result is near ±20 mV [31] as the polydispersity index and zeta potential of nanosuspensions dictate its stability [32]. The obtained nanosuspension is expected to be stable since the polydispersity index was 1.177 ± 0.22 and the zeta potential was negative for all batches (−21.3 ± 4.61 mV), this result is in accordance with previous study, for this kind of formulation [32]. The high value for zeta potential conferred electrostatic stability to the suspended particles, minimizing the effects of aggregation and deposition [33]. The prevention of particles aggregation along, allows the permeation of the bioactive agents trough the root canal system [28,29]. The anti-inflammatory effect of IndOH-NC suspension was already reported in previous study in acute and chronic inflammation processes, even in sub-therapeutic doses, providing a gastrointestinal safe therapeutic alternative for this medication [18]. The data reported in that study demonstrated that polymeric nanocapsules are able to successfully carry indomethacin into the inflammation sites. The utilization of IndOH-NC in dental materials was also reported by some authors, with the aim of providing agents that act on the inflammatory process of pulp tissue, through dental adhesives [24]. Thus, the IndOH-NC suspension present on this study appears to be an alternative treatment of inflammatory situations found in pulp infection to complete the periapical repair, as it only occurs once the antigen is neutralized during the inflammatory response [34].

One of the main advantages of the release of amoxicillin at the local site is that *E. faecalis* is a persistent microorganism, and the major responsible by endodontic treatment failures [35], present in over one third of the root canals with persisting periapical lesions [36]. In certain cases, antibiotics are not effective because of shortcomings caused by physiological barriers or due to the inadequate blood supply at the local area, therefore, the concentration of antibiotics administered systemically may not be sufficient to achieve a desirable local concentration of the drug [14,37]. Moreover, the individual resistance to antimicrobials is a continually evolving global issue. Hospital-acquired infections are caused by antimicrobial-resistant pathogens in more than 21% of the cases, this outcome was equal to 2 million cases of infections with an estimated 23.000 deaths, as is shown on the most recent epidemiologic data on antimicrobial-resistant organisms in the USA, by the Center for Disease Control and Prevention (CDC, United States, U.S. Department of Health and Human Services). Such problems prevenient from systemically administration of antibiotics, are thought to be minimized by the development of controlled release systems [37], as the one developed in this study, which involves the implantation of antibiotic loaded polymeric systems directly to the site of infection and consequently, lowering the amount of amoxicillin needed to achieve the desired antibacterial effect.

The amoxicillin delivery by polymeric devices has already demonstrated its efficacy against *E. faecalis* in a previous study [13] and, as shown in Table 3, the experimental paste demonstrated an inhibition zone higher than all the other materials tested ($p < 0.05$). Also, The GP group was capable of forming an inhibition halo, and this fact can be attributed to the presence of neomycin on the material's composition. The results of ADT indicated no (or low) antibacterial activity for UL group. The reason of this inability can be related to the low permeation ability of this calcium hydroxide-based material, which is in accordance with previous studies comparing different endodontic materials against *E. faecalis* [38].

The *E. faecalis* is often found in planktonic state in the oral cavity, mainly because in this form the microorganism has a greater chance to permeate in the root canal system than if a biomembrane structure (biofilm) is formed, leading to an endodontic retreatment necessity [39]. According to the antibacterial activity against the planktonic cells evaluated in this study, the GP and UL groups showed no significant difference from negative control group. The only group to present antibacterial activity against planktonic bacteria was the experimental paste developed ($p < 0.05$). Also, the HPMC present on the synthesis of the AMX-MS is already known to be one of the most commonly used hydrophilic biodegradable polymers in the development of controlled release formulations [29] approved by the United States Food and Drug Administration (FDA). The HPMC can also attribute to the experimental paste a sustained release of the amoxicillin, as the utilization of antibiotics is an essential method for the treatment of bacterial infections in Dentistry [14].

The effects of the materials were further analyzed by cell assays as these materials take direct contact with different cell types, such as dental pulp cells, dental follicle cells and periodontal ligament cells [40]. The three endodontic materials (EX, GP and UL) were evaluated regarding citocompatibility and bioactivity on fibroblastic cell line due its participation in periapical repair [41]. As seen in the viability graph results (Fig. 3), the greatest cytotoxic effect was shown in MTT assay, while for SRB all materials presented suitable values regarding viability. The mitochondrial dehydrogenases presented in the reduction process of MTT assay is expressed only in vital cells and it is inactivated right after cell death [42]. The SRB assay relies on the binding to basic amino acids under mild acidic conditions, while the stain is released under basic conditions [43]. As the resulting products of SRB is in a stoichiometric relationship with the chemical process, the amount of dye extracted from stained cells is directly proportional to the cell mass on the quantification of desired data. This type of SRB binding eliminates the influence of varying the intrinsic cell biological specifications on the quantification process [44], conferring this assay a trustful cell enumeration method, as it does not entrust on the cell metabolic rate or the activity of only live cells. The calcium hydroxide-based paste presented the higher results regarding viability, other materials based on calcium hydroxide were also investigated and similar results to this study were found [45]. Despite the cytotoxic effect present on MTT assay for the 10% conditioned medium

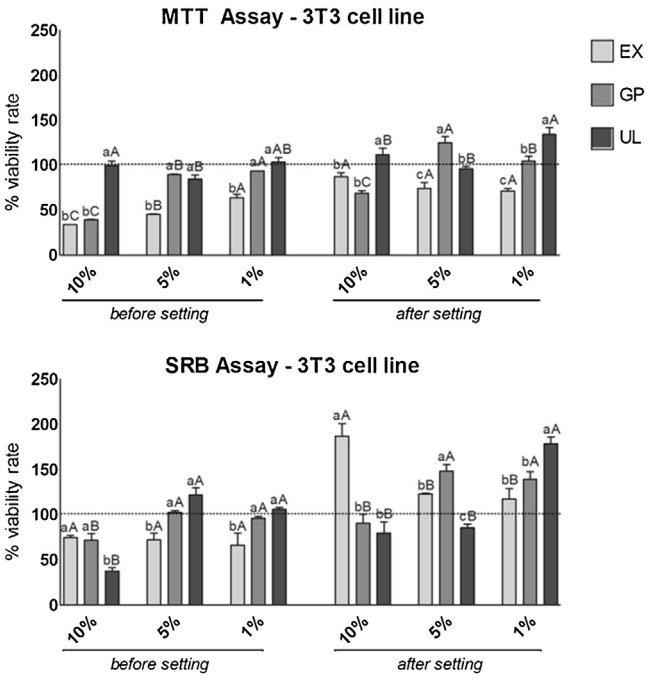

Fig. 3 – Cell viability of extracts with different concentrations (1, 5, 10%) derived from the tested materials after 24 h of setting and the fresh pastes. The results show mean and standard deviation of experiments performed in triplicate. Different capital letters represent statistical differences at the same material in different concentrations. Different lowercase letters represent statistical differences between the materials at the same concentration.

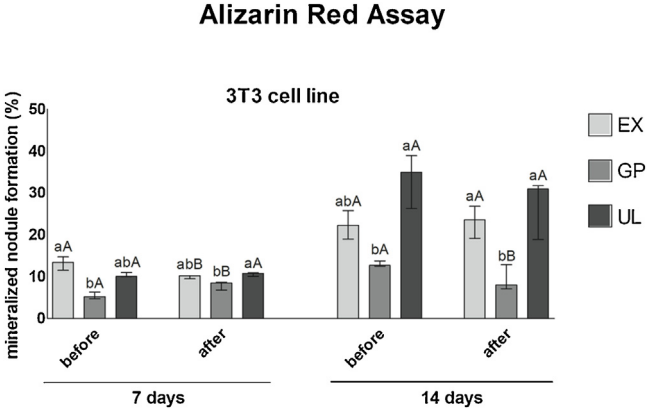

Fig. 4 – Quantitative analysis of mineralized nodules after 7 and 14 days in culture. Data reported as mean and standard deviation performed in triplicate. Different lowercase represent statistical differences between the materials before or after setting. Different capital letters represent statistical difference at the same material before and after setting.

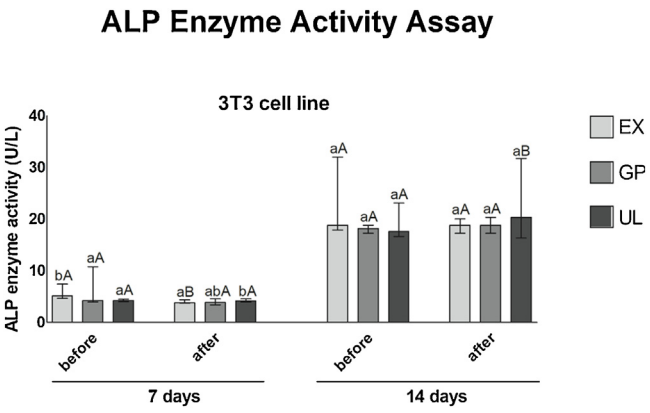

Fig. 5 – ALP enzyme activity after cells exposure to different materials after 7 and 14 days in culture. Data reported as mean and standard deviation performed in triplicate. Different lowercase represent statistical differences between the materials before or after setting. Different capital letters represent statistical difference at the same material before and after setting.

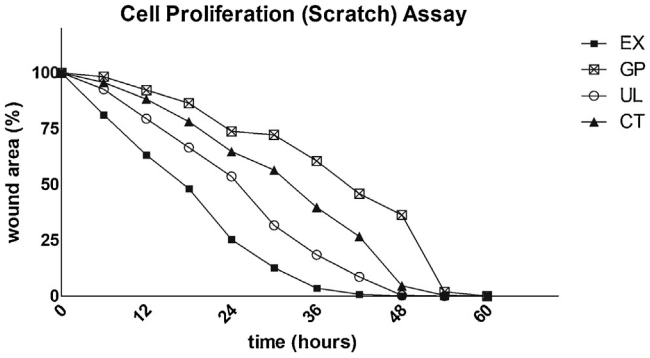

Fig. 6 – The cellular migration ability of fibroblasts exposed to materials extracts as evaluated by an in vitro scratch wound-healing model. Confluent monolayer of cells were wounded and treated with extracts until complete closure. Every material was different from each other and from the control group at the final closure of the wound ($p < 0.05$).

concentration of the experimental endodontic paste, it should be take in consideration the limitations of this test, as well the short length of the incubation period (24 h), the number of viable cells and their metabolic activity. The values for SRB assay showed greater compatibility for the experimental paste and 70% or more of cell viability is within the ISO 10993-5 standards. The association of both cell proliferation assays is advised to avoid false-positive results [43].

As expected, the paste composed of calcium phosphate, calcium tungstate, amoxicillin, and indomethacin take advantage in primary teeth as an filling material for presenting lower cytotoxicity when compared with camphorated paramonochlorophenol [8] and in regenerative treatment when compared with triple antibiotic paste on account of the minocycline that binds to calcium ions and form an insoluble complex [10,11]. Besides, presented bioactivity to improve the regeneration of the damaged apical periodontal attachment and surrounding bone.

For the osteogenic potential, the Alizarin Red S assay revealed statistically lower results of mineralized nodules formation for GP paste compared to the other materials. Since the iodoform-based paste does not have any component that could release ions Ca^{+2} and/or PO_4^{3-} to the culture

medium, bioactivity was very unlikely to occur through ion-by-ion deposition. When exposed to aqueous solution, the α-TCP present on the experimental paste can supply Ca^{2+} and PO_4^{3-} and, as a result of consecutive dissolution-precipitation reactions, Ca-deficient apatite crystals precipitation is forthcoming to appear [46], clarifying the results found for bioactivity assays on this study. Materials that are prone to release calcium ions such as calcium hydroxide-based materials [47], calcium silicate-based [48], bioactive glasses [49] and calcium phosphates derivates [12,50,51] after ionic dissolution can provide a more favorable biomimetic microenvironment for deposition of mineral via ion-by-ion release, forming hydroxyapatite nucleation sites [52].

Nucleation is the first step in biomineralization and plays an important role in building up a novel mineralized structure [53], the apatite deposition of tricalcium-phosphate based materials suggests that bioactive composites could enhance healing in periapical tissues [12]. Deposition of inorganic particles at the root canal surface can also occur during the degradation process of the radiopaque fillers, such as the calcium tungstate utilized in this study, increasing the sealing ability [29].

Other materials that are commonly used in dental practice for endodontic healing are the calcium silicate–based materials (CSMs), such as mineral trioxide aggregate (MTA). Although it is already known MTA sealing ability, biocompatibility, and regenerative capabilities [54,55], some studies indicate that these materials can dissolve the components of the mineralized dentin matrix [56,57], mainly due to its high pH after setting and the formation of saturated $Ca(OH)_2$ along the walls of the root canal [58]. Apparently, the saturated $Ca(OH)_2$ (molecular weight, 56.1 Da) alter the elastic modulus of mineralized dentin [58] and, because of their small sizes, it is possible that these highly alkaline inorganic molecules penetrates the intrafibrillar congregates of mineralized collagen fibrils reshaping the tropocollagen 3D conformation [57]. It should be considered that endodontic retreatment remodel the root canal walls, hence that CSMs aren't recommended to obturate root canals with thin dentinal walls, to avoid collagen degradation that might lead to fractures [56,57]. The saturated $Ca(OH)_2$ present on the dissolution of MTA isn't expected for the experimental endontic paste of the present study. Furthermore, it is possible that the EX paste promotes ions Ca^{2+} and PO_4^{3-} release prevenient from the α-TCP composition [59], and due to the dissolution of such ions, bioactivity by signaling for cell function and differentiation is favored. In addition, the dissolution of these ions from the EX paste can also act as building blocks for hydroxyapatite mineralization by the precipitation of Ca-deficient apatite crystal along the walls of the root canal [46,54].

Bioactivity can also be measured by the ALP enzyme function, as it is a recognized marker of cell differentiation into osteoblasts and a fundamental enzyme in nucleation process of hydroxyapatite [60,61]. Therefore, the evaluation of this enzyme allows the determination of the materials bioactivity and the potential to promote tissue repair. The increase in ALP activity was consistent with the significant high number of ARS-stained nodules observed at the 14 days period of cell culture for evaluated groups, the increasing in ion leaching for UL and EX groups may be related with increased results for cell mineralization in the present study. The ALP and ARS results can be justified by the ability of fibroblasts cells to differentiate into cells that secrete mineralized matrix [62], moreover, it was already revealed by some authors that the presence of apatite-like crystals is a stimulator of cellular adhesion and migration of fibroblasts cells *in vitro* [63]. Additional to ALP and ARS assays, the effect of materials extracts on cellular migration of fibroblastic cell line was determined using a scratch wound healing model. One advantage of this method is the possibility to understand to some extent the migration of cells *in vivo* [64]. Treatment with all materials promoted cell migration, and the rate of wound closure shows accordance with the previous results of this study for osteogenic potential and citocompatibility.

Adhesion and migration of fibroblastic cells are key phenomena during the initial stages of tooth related problems, because its participation on local tissue repairs in a variety of physiological and pathological conditions [40,65]. The release of calcium ions is an important factor for cell signaling, regulating essential functions for the cell attachment, migration, differentiation and proliferation of hard tissue-producing cells, the release of Ca^{2+} ion for UL and EX groups may explain the best results for these groups on the wound healing of the scratch [66]. Along with the results of cell migration, it has been shown in this study that the experimental endodontic paste could accelerate the process of cell migration for fibroblasts in comparison to other tested materials, with complete wound closure around 42 h ($p < 0.05$). As the conditioned medium of the materials were utilized in clinically similar conditions (right after mixing), this type of research protocol employed may predict better the *in vivo* effect of the materials in the cell assays [67], providing reliable results. These results, in combination with suitable physical properties, may be responsible for the outcome in increased differentiation rates found in cell studies for the experimental material.

5. Conclusion

The present study successfully synthesized an experimental endodontic paste showing suitable physical and biological properties. The association of bioactive agents with controlled release resulted in the ability to stimulate nucleation sites for the formation of apatite crystals nodules and enhanced osteogenic activity over time. Furthermore, the antibacterial effect and citocompatibility can allow the active components to provide a more effective regeneration of periapical tissue.

Acknowledgements

The authors gratefully acknowledge Coordenação de Aperfeiçoamento de Pessoal de Nível Superior (CAPES, Brazil) for the scholarship of CUPPINI M and Centro de Microscopia e Microanálise (CMM, Universidade Federal do Rio Grande do Sul).

REFERENCES

[1] Smith CS, Setchell DJ, Harty FJ. Factors influencing the success of conventional root canal therapy—a five year retrospective study. Int Endod J 1993;26:321–33.

[2] Bystrom A, Sundqvist G. Bacteriologic evaluation of the efficacy of mechanical root canal instrumentation in endodontic therapy. Scand J Dent Res 1981;89:321–8.

[3] Estrela C, Sydney GB, Bammann LL, Felippe Jr O. Mechanism of action of calcium and hydroxyl ions of calcium hydroxide on tissue and bacteria. Braz Dent J 1995;6:85–90.

[4] AAPD. Council on Clinical Affairs. Guideline on pulp therapy for primary and immature permanent teeth. Clin Pract Guidelines 2016/2017;38:280–8.

[5] Cogulu D, Uzel A, Oncag O, Eronat C. PCR-based identification of selected pathogens associated with endodontic infections in deciduous and permanent teeth. Oral Surg Oral Med Oral Pathol Oral Radiol Endod 2008;106:443–9.

[6] Evans M, Davies JK, Sundqvist G, Figdor D. Mechanisms involved in the resistance of *Enterococcus faecalis* to calcium hydroxide. Int Endod J 2002;35:221–8.

[7] Cerqueira DF, Mello-Moura AC, Santos EM, Guedes-Pinto AC. Cytotoxicity, histopathological, microbiological and clinical aspects of an endodontic iodoform-based paste used in pediatric dentistry: a review. J Clin Pediatr Dent 2008;32:105–10.

[8] Soekanto A, Kasugai S, Mataki S, Ohya K, Ogura H. Toxicity of camphorated phenol and camphorated parachlorophenol in dental pulp cell culture. J Endod 1996;22:284–6.

[9] Jacobs JC, Troxel A, Ehrlich Y, Spolnik K, Bringas JS, Gregory RL, et al. Antibacterial effects of antimicrobials used in regenerative endodontics against biofilm bacteria obtained from mature and immature teeth with necrotic pulps. J Endod 2017;43:575–9.

[10] Kim J, Kim Y, Shin S, Park J, Jung I. Tooth discoloration of immature permanent incisor associated with triple antibiotic therapy: a case report. J Endod 2010;36:1086–91.

[11] Tanase S, Tsuchiya H, Yao J, Ohmoto S, Takagi N, Yoshida S. Reversed-phase ion-pair chromatographic analysis of tetracycline antibiotics: application to discolored teeth. J Chromatogr B Biomed Sci Appl 1998;706:279–85.

[12] Dornelles NBJ, Collares FM, Genari B, de Souza Balbinot G, Samuel SMW, Arthur RA, et al. Influence of the addition of microsphere load amoxicillin in the physical, chemical and biological properties of an experimental endodontic sealer. J Dent 2018;68:28–33.

[13] Portella FF, Collares FM, dos Santos LA, dos Santos BP, Camassola M, Leitune VC, et al. Glycerol salicylate-based containing alpha-tricalcium phosphate as a bioactive root canal sealer. J Biomed Mater Res B Appl Biomater 2015;103:1663–9.

[14] Molander A, Reit C, Dahlen G, Kvist T. Microbiological status of root-filled teeth with apical periodontitis. Int Endod J 1998;31:1–7.

[15] Vega-González A, Domingo C, Elvira C, Subra P. Precipitation of PMMA/PCL blends using supercritical carbon dioxide. J Appl Polym Sci 2004;91:2422–6.

[16] Dimer FA, Ortiz M, Pase CS, Roversi K, Friedrich RB, Pohlmann AR, et al. Nanoencapsulation of olanzapine increases its efficacy in antipsychotic treatment and reduces adverse effects. J Biomed Nanotechnol 2014;10:1137–45.

[17] Portella FF, Santos PD, Lima GB, Leitune VC, Petzhold CL, Collares FM, et al. Synthesis and characterization of a glycerol salicylate resin for bioactive root canal sealers. Int Endod J 2014;47:339–45.

[18] Bernardi A, Zilberstein AC, Jager E, Campos MM, Morrone FB, Calixto JB, et al. Effects of indomethacin-loaded nanocapsules in experimental models of inflammation in rats. Br J Pharmacol 2009;158:1104–11.

[19] Raval JA, Patel JK, Patel MM. Formulation and in vitro characterization of spray dried microspheres of amoxicillin. Acta Pharm 2010;60:455–65.

[20] Kumar R, Singh A, Garg N, Siril PF. Solid lipid nanoparticles for the controlled delivery of poorly water soluble non-steroidal anti-inflammatory drugs. Ultrason Sonochem 2018;40:686–96.

[21] Zanotto-Filho A, Coradini K, Braganhol E, Schroder R, de Oliveira CM, Simoes-Pires A, et al. Curcumin-loaded lipid-core nanocapsules as a strategy to improve pharmacological efficacy of curcumin in glioma treatment. Eur J Pharm Biopharm 2013;83:156–67.

[22] LeGeros RZ. Calcium phosphate-based osteoinductive materials. Chem Rev 2008;108:4742–53.

[23] Fessi H, Puisieux F, Devissaguet JP, Ammoury N, Benita S. Nanocapsule formation by interfacial polymer deposition following solvent displacement. Int J Pharm 1989;55:R1–4.

[24] Genari B, Leitune VC, Jornada DS, Camassola M, Pohlmann AR, Guterres SS, et al. Effect of indomethacin-loaded nanocapsules incorporation in a dentin adhesive resin. Clin Oral Investig 2017;21:437–46.

[25] Thurmer MB, Vieira RS, Fernandes JM, Coelho WTG, dos Santos LA. Synthesis of alpha-tricalcium phosphate by wet reaction and evaluation of mechanical properties. Mater Sci Forum 2012;727–728:1164–9.

[26] Venturini CG, Jäger E, Oliveira CP, Bernardi A, Battastini AMO, Guterres SS, et al. Formulation of lipid core nanocapsules. Colloids Surf A Physicochem Eng Asp 2011;375:200–8.

[27] de Deus GA, Martins F, Lima AC, Gurgel-Filho ED, Maniglia CF, Coutinho-Filho T. Analysis of the film thickness of a root canal sealer following three obturation techniques. Pesqui Odontol Bras 2003;17:119–25.

[28] Razmi H, Ashofteh Yazdi K, Jabalameli F, Parvizi S. Antimicrobial effects of AH26 sealer/antibiotic combinations against *Enterococcus faecalis*. Iran Endod J 2008;3:103–8.

[29] Collares FM, Leitune VC, Rostirolla FV, Trommer RM, Bergmann CP, Samuel SM. Nanostructured hydroxyapatite as filler for methacrylate-based root canal sealers. Int Endod J 2012;45:63–7.

[30] Tanomaru JM, Cezare L, Goncalves M, Tanomaru Filho M. Evaluation of the radiopacity of root canal sealers by digitization of radiographic images. J Appl Oral Sci 2004;12:355–7.

[31] Patravale VB, Date AA, Kulkarni RM. Nanosuspensions: a promising drug delivery strategy. J Pharm Pharmacol 2004;56:827–40.

[32] Ahuja M, Dhake AS, Sharma SK, Majumdar DK. Diclofenac-loaded Eudragit S100 nanosuspension for ophthalmic delivery. J Microencapsul 2011;28:37–45.

[33] Harmata AJ, Guelcher SA. 3 – Effects of surface modification on polymeric biocomposites for orthopedic applications. In: Huinan L, editor. Nanocomposites for musculoskeletal tissue regeneration. Oxford: Woodhead Publishing; 2016. p. 67–91.

[34] Holland R, Gomes JEF, Cintra LTA, Queiroz IOA, Estrela C. Factors affecting the periapical healing process of endodontically treated teeth. J Appl Oral Sci 2017;25:465–76.

[35] Hoelscher AA, Bahcall JK, Maki JS. In vitro evaluation of the antimicrobial effects of a root canal sealer-antibiotic combination against *Enterococcus faecalis*. J Endod 2006;32:145–7.

[36] Rocas IN, Siqueira Jr JF, Santos KR. Association of *Enterococcus faecalis* with different forms of periradicular diseases. J Endod 2004;30:315–20.

[37] Mahmoudian M, Ganji F. Vancomycin-loaded HPMC microparticles embedded within injectable thermosensitive chitosan hydrogels. Prog Biomater 2017;6:49–56.
[38] Poggio C, Trovati F, Ceci M, Colombo M, Pietrocola G. Antibacterial activity of different root canal sealers against *Enterococcus faecalis*. J Clin Exp Dent 2017;9:e743–8.
[39] Wang QQ, Zhang CF, Chu CH, Zhu XF. Prevalence of *Enterococcus faecalis* in saliva and filled root canals of teeth associated with apical periodontitis. Int J Oral Sci 2012;4:19–23.
[40] Mestieri LB, Gomes-Cornelio AL, Rodrigues EM, Faria G, Guerreiro-Tanomaru JM, Tanomaru-Filho M. Cytotoxicity and bioactivity of calcium silicate cements combined with niobium oxide in different cell lines. Braz Dent J 2017;28:65–71.
[41] Willershausen B, Marroquin BB, Schafer D, Schulze R. Cytotoxicity of root canal filling materials to three different human cell lines. J Endod 2000;26:703–7.
[42] Eid AA, Gosier JL, Primus CM, Hammond BD, Susin LF, Pashley DH, et al. In vitro biocompatibility and oxidative stress profiles of different hydraulic calcium silicate cements. J Endod 2014;40:255–60.
[43] Vichai V, Kirtikara K. Sulforhodamine B colorimetric assay for cytotoxicity screening. Nat Protoc 2006;1:1112–6.
[44] van Tonder A, Joubert AM, Cromarty AD. Limitations of the 3-(4,5-dimethylthiazol-2-yl)-2,5-diphenyl-2*H*-tetrazolium bromide (MTT) assay when compared to three commonly used cell enumeration assays. BMC Res Notes 2015; 8:47.
[45] Luczaj-Cepowicz E, Marczuk-Kolada G, Pawinska M, Obidzinska M, Holownia A. Evaluation of cytotoxicity and pH changes generated by various dental pulp capping materials – an in vitro study. Folia Histochem Cyto 2017;55:86–93.
[46] TenHuisen KS, Brown PW. Formation of calcium-deficient hydroxyapatite from alpha-tricalcium phosphate. Biomaterials 1998;19:2209–17.
[47] Gandolfi MG, Siboni F, Botero T, Bossu M, Riccitiello F, Prati C. Calcium silicate and calcium hydroxide materials for pulp capping: biointeractivity, porosity, solubility and bioactivity of current formulations. J Appl Biomater Funct Mater 2015;13:43–60.
[48] Camilleri J, Formosa L, Damidot D. The setting characteristics of MTA plus in different environmental conditions. Int Endod J 2013;46:831–40.
[49] Hench LL, Xynos ID, Polak JM. Bioactive glasses for in situ tissue regeneration. J Biomater Sci Polym Ed 2004;15:543–62.
[50] Weir MD, Ruan J, Zhang N, Chow LC, Zhang K, Chang X, et al. Effect of calcium phosphate nanocomposite on in vitro remineralization of human dentin lesions. Dent Mater 2017;33:1033–44.
[51] Collares FM, Leitune VCB, Portella FF, Santos PD, Balbinot GS, Dos Santos LA, et al. Methacrylate-based root canal sealer containing chlorexidine and alpha-tricalcium phosphate. J Biomed Mater Res B Appl Biomater 2017:1439–1443.
[52] Dai L, Liu Y, Salameh Z, Khan S, Mao J, Pashley DH, et al. Can caries-affected dentin be completely remineralized by guided tissue remineralization? Dent Hypotheses 2011;2:74–82.
[53] Jiang H, Liu XY. Principles of mimicking and engineering the self-organized structure of hard tissues. J Biol Chem 2004;279:41286–93.
[54] Camilleri J. Evaluation of the effect of intrinsic material properties and ambient conditions on the dimensional stability of white mineral trioxide aggregate and Portland cement. J Endod 2011;37:239–45.
[55] Camilleri J. Characterization of hydration products of mineral trioxide aggregate. Int Endod J 2008;41:408–17.
[56] Sawyer AN, Nikonov SY, Pancio AK, Niu L, Agee KA, Loushine RJ, et al. Effects of calcium silicate-based materials on the flexural properties of dentin. J Endod 2012;38:680–3.
[57] Leiendecker AP, Qi Y, Sawyer AN, Niu L, Agee KA, Loushine RJ, et al. Effects of calcium silicate-based materials on collagen matrix integrity of mineralized dentin. J Endod 2012;38:829–33.
[58] Grigoratos D, Knowles J, Ng Y-L, Gulabivala K. Effect of exposing dentine to sodium hypochlorite and calcium hydroxide on its flexural strength and elastic modulus. Int Endod J 2001;34:113–9.
[59] Dorozhkin SV. Calcium orthophosphate deposits: preparation, properties and biomedical applications. Mater Sci Eng C 2015;55:272–326.
[60] Varalakshmi PR, Kavitha M, Govindan R, Narasimhan S. Effect of statins with alpha-tricalcium phosphate on proliferation, differentiation, and mineralization of human dental pulp cells. J Endod 2013;39:806–12.
[61] Salles LP, Gomes-Cornelio AL, Guimaraes FC, Herrera BS, Bao SN, Rossa-Junior C, et al. Mineral trioxide aggregate-based endodontic sealer stimulates hydroxyapatite nucleation in human osteoblast-like cell culture. J Endod 2012;38:971–6.
[62] Murakami Y, Kojima T, Nagasawa T, Kobayashi H, Ishikawa I. Novel isolation of alkaline phosphatase-positive subpopulation from periodontal ligament fibroblasts. J Periodontol 2003;74:780–6.
[63] Kasaj A, Willershausen B, Junker R, Stratul SI, Schmidt M. Human periodontal ligament fibroblasts stimulated by nanocrystalline hydroxyapatite paste or enamel matrix derivative. An in vitro assessment of PDL attachment, migration, and proliferation. Clin Oral Investig 2012;16:745–54.
[64] Liang CC, Park AY, Guan JL. In vitro scratch assay: a convenient and inexpensive method for analysis of cell migration in vitro. Nat Protoc 2007;2:329–33.
[65] Keatch RP, Schor AM, Vorstius JB, Schor SL. Biomaterials in regenerative medicine: engineering to recapitulate the natural. Curr Opin Biotechnol 2012;23:579–82.
[66] Tanomaru-Filho M, Andrade AS, Rodrigues EM, Viola KS, Faria G, Camilleri J, et al. Biocompatibility and mineralized nodule formation of Neo MTA Plus and an experimental tricalcium silicate cement containing tantalum oxide. Int Endod J 2017;2:e31–9.
[67] Pedano MS, Li X, Li Shuchen, Sun Z, Cokic SM, Putzeys E, et al. Freshly-mixed and setting calcium-silicate cements stimulate human dental pulp cells. Dent Mater 2018;17:31155–7.